ICROS-SICE International Joint Conference 2009
August 18-21, 2009, Fukuoka International Congress Center, Japan

Modeling of Rebound Phenomenon between Ball and Racket Rubber with Spinning Effect

Akira Nakashima[1], Yosuke Kobayashi[1], Yuki Ogawa[1] and Yoshikazu Hayakawa[1,2]

[1]Dept. of Mechanical Science and Engineering, Graduate School of Engineering, Nagoya University, Nagoya, Japan
(Tel: +81-52-789-2746; E-mail: a_nakashima@nuem.nagoya-u.ac.jp)
[2]RIKEN-TRI Collaboration Center, RIKEN, 2271-103, Anagahora, Shimoshidami, Moriyama-ku, Nagoya, Japan

Abstract: We model the rebound phenomenon between a ping-pong ball and the table/racket rubber. In the model between the ball and racket rubber, it is assumed that the kinetic energy of the contact velocity is stored as the potential energy due to the elasticity of the rubber. This assumption leads to that the impulse in the horizontal direction is proportional to the contact velocity. The vertical and horizontal COR in the models of the table and rubber are identified with the measured velocity and spin of the ball by high-speed vision sensors. The models are verified by other experimental data.

Keywords: Rebound phenomenon, Racket rubber, Vision sensors

1. INTRODUCTION

We aim to realize a robot to play table tennis with a human as a typical example of robots in uncertain environment since playing table tennis is a dexterous task for humans. For simplicity, consider the situation of Fig. 1, where a robot tries to hit a flying ball. In this situation, the strategy of the robot playing table tennis can be decomposed as the following subtasks: 1) To detect the states of the flying ball with vision sensors; 2) To predict the ball trajectory; 3) To determine the trajectory of the racket attached to the robot for the hit ball to achieve desired trajectory. The number 1) means the image processing algorithm to obtain the position, the translational and rotational velocities of the ball. The number 2) means the prediction of the position and translational/rotational velocities of the ball for the next task of the determination. The number 3) means the determination of the trajectories of the position and orientation of the racket attached to the robot for the ball to follow desired trajectory. In the subtasks 2) and 3), the ball *rebounds* from the table and the racket rubber. It is therefore necessary to model the rebound phenomenon between the ball and the table/rubber in order to achieve the subtasks 2) and 3).

The rebound phenomenon between a ball and a surface has been studied by many researchers. Garwin [1] proposed the coefficient of restitution (COR) in the direction *parallel* to the surface. He determined from experimental data which the contact is the rolling, sliding or both together during the impact and whether the kinetic energy is stored as elastic one or not. Brody [2] considered the effect of *friction* of the surface with the assumption of no compression of the ball. He derived the condition of the rolling contact which is related to the translational and rotational velocities just before the rebound. Shibukawa [3] derived the condition which determines whether the rolling contact happens or not during the impact. As specified situations of the rebound, R. Cross [4] considered the effect of friction between the ball and strings in tennis. He also considered other situations, e.g., the horizontal COR between balls of various properties and a solid surface [5]. Furthermore, he investigated the bounce of a spinning ball being incident near the normal to the surface as an example of situations of hitting a ball by a racket because this situation was not investigated [6]. For the normal COR, R. Cross [7] investigated the relation between the normal COR and the dynamics hysteresis of the impact force. Kawazoe [8] modeled the normal COR of a table tennis rubber as a linear function of the velocity just before the rebound, which shows the dissipation of the elastic energy. In these studies, the elastic properties of the ball and surface were not considered analytically or evaluated as the values of coefficients on restitution experimentally.

Fig. 1 A robot try to hit a flying ball.

We model the rebound phenomenon between a ping-pong ball and the table/racket rubber. The model between the ball and table is the generalized one of Shibukawa's model [3]. In the model between the ball and racket rubber, it is assumed that the kinetic energy of the contact velocity is stored as the potential energy due to the elasticity of the rubber. This assumption leads to that the impulse in the horizontal direction is proportional to the contact velocity. The vertical and horizontal COR in the models of the table and rubber are identified with the measured velocity and spin of the ball by high-speed vision sensors. The models are verified by other experimental data.

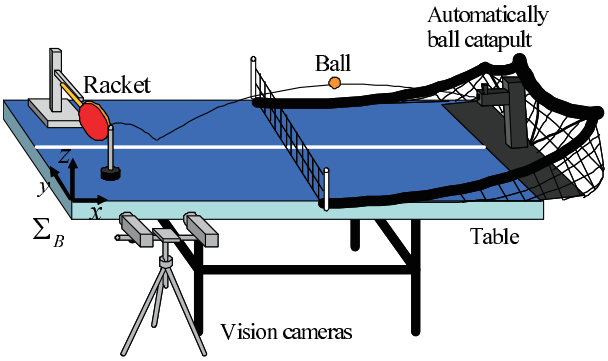

Fig. 2 Experimental system.

2. EXPERIMENTAL SYSTEM AND BALL DETECTION

Fig. 2 shows the experimental system for detecting the ball states. The table tennis is an international standard one whose size is 1525(W)×760(H)×2740(D) [m]. The ball is shot out from the automatic ball catapult ROBOPONG 2040 (SAN-EI Co.) which is set at the end of the table. The parameters of the ball are $m = 2.7 \times 10^{-3}$[kg] and $r = 2.0 \times 10^{-2}$[m]. The flying ball is measured by the high-speed vision sensors with 1000 [fps] (Hamamatsu Photonics K.K.). The array and pixel sizes are 232×232 and 2.9×10^{-5} [pixel/m]. The sampled data are quantized as 2D image data with the monochrome brightness of 8bit (0–255). The focal length of the lens is 3.5×10^{-2} [m]. Σ_B is the reference frame. The racket is an usual one (Butterfly K.K.) and is fixed at the table whose surface is normal to the x-axis of Σ_B. The cameras are calibrated with respect to Σ_B. The 3D position in Σ_B can be therefore calculated with the corresponding 2D image positions of the two cameras [9].

By this experimental system, we get the translational and rotational velocities of the ball for the modeling of the rebound phenomenon. It is assumed that there is no effect of the air resistance. By this assumption, the translational and rotational velocities of the ball are constants when the ball is flying freely. Here, the image processing and detection of the 2D image data of the two cameras are described with respect to the only one because

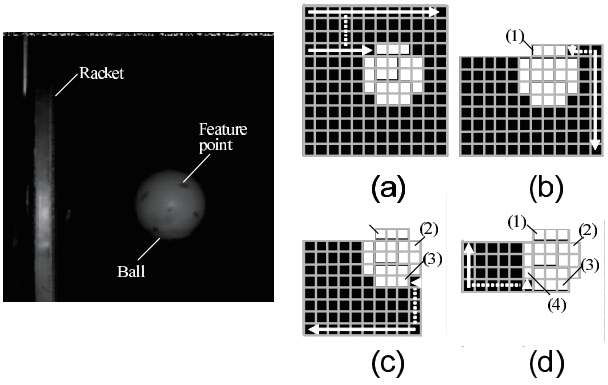

Fig. 3 Image data and Detection of the center of the ball.

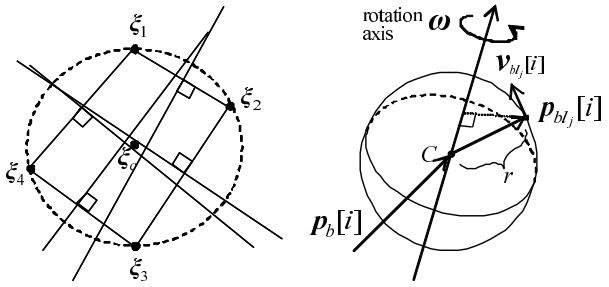

Fig. 4 Detection of the translation and rotation velocities.

they are the same as the other one. The left of Fig. 3 shows an example of the image data of the camera. Let us consider the detection of the center of the ball. Since the ball is white and the background is much darker than the ball, all the area of the ball can be easily detected by the simple scanning shown in the right of Fig. 3. In the scanning of (a), the arrows are scanned in turn from the left and top until the brightness of the scanned image is larger than a specified threshold. The scanning of (b)–(d) are similar to the one of (a). The positions of the detected data with the threshold are recorded as $\boldsymbol{\xi}_i := (u_i, v_i) \in \mathbb{R}^2$ $(i = 1, \cdots, 4)$. Consider the mediators of the lines between $\boldsymbol{\xi}_{i+1}$ and $\boldsymbol{\xi}_i$ $(i = 1, \cdots, 4)$, $\boldsymbol{\xi}_5 := \boldsymbol{\xi}_1$ as shown in the left of Fig. 4. Define $\boldsymbol{\xi}_c$ as the center of the ball. The center $\boldsymbol{\xi}_c$ is obtained by the least squares method with the following performance function:

$$V_c(\boldsymbol{\xi}) := \sum_{i=1}^{4} \frac{\left|(\boldsymbol{\xi}_{i+1} - \boldsymbol{\xi}_i)^{\mathrm{T}} \boldsymbol{\xi}_c - \frac{1}{2}(\|\boldsymbol{\xi}_{i+1}\|^2 - \|\boldsymbol{\xi}_i\|^2)\right|^2}{\|\boldsymbol{\xi}_{i+1} - \boldsymbol{\xi}_i\|^2}, \tag{1}$$

which is the sum of the squares of the distances of $\boldsymbol{\xi}$ from the mediators. Define $\boldsymbol{p}_b \in \mathbb{R}^3$ as the corresponding 3D position vector of $\boldsymbol{\xi}_c \in \mathbb{R}^2$. The translational velocities of the ball just before and after the rebound are obtained by the mean of all the velocities between the $(i+1)$th and ith position as

$$\boldsymbol{v}_b = \frac{\sum_{i=0}^{N-2} \boldsymbol{v}_b[i]}{N-1}, \ \boldsymbol{v}_b[i] := \frac{\boldsymbol{p}_b[i+1] - \boldsymbol{p}_b[i]}{\Delta t}, \tag{2}$$

where $\Delta t = 1$[ms] is the sampling time and N is the number of the frames before or after the rebound. Note that $[i]$ denotes the $(i+1)$th frame.

Next, consider the detection of the rotational velocity of the ball. The right of Fig. 4 shows the ball in the ith frame, where $\boldsymbol{\omega} \in \mathbb{R}^3$ is the rotation axis, $\boldsymbol{p}_{bl_j} := \boldsymbol{p}_{l_j} - \boldsymbol{p}_b$ and $\boldsymbol{p}_{l_j} \in \mathbb{R}^3$ is the feature point on the ball $(j = 1, \cdots, N_l)$. For the $j$the feature point, the following rotational relationship is hold [10]:

$$\boldsymbol{p}_{bl_j}[i+1] = e^{\widehat{\omega}\Delta t} \boldsymbol{p}_{bl_j}[i], \ e^{\widehat{\omega}\Delta t} \approx \boldsymbol{I}_3 + \widehat{\boldsymbol{\omega}}\Delta t, \tag{3}$$

where $\widehat{\boldsymbol{\omega}} \in \mathbb{R}^{3\times3}$ is the skew-symmetric matrix which is corresponding the cross product of $\boldsymbol{\omega}$ and $e^{\widehat{\omega}\Delta t}$ is linearized because of the small Δt. (3) is rewritten as

$$\widehat{\boldsymbol{p}}_{bl_j}[i]\boldsymbol{\omega} = -\boldsymbol{v}_{bl_j}[i], \boldsymbol{v}_{bl_j}[i] := \frac{\boldsymbol{p}_{bl_j}[i+1] - \boldsymbol{p}_{bl_j}[i]}{\Delta t}. \tag{4}$$

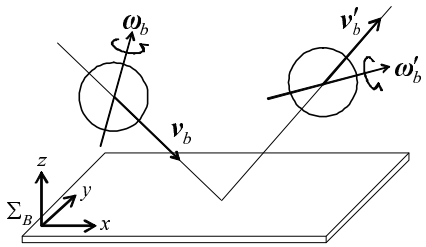

Fig. 5 Ball velocities just before and after the rebound.

If the direction of $\boldsymbol{\omega}$ is given, (4) can be rewritten as

$$\theta_\omega = \frac{\|\boldsymbol{v}_{bl_j}[i]\|}{\|\boldsymbol{p}_{bl_j}[i] \times \boldsymbol{n}_\omega\|}, \tag{5}$$

where $\boldsymbol{\omega} := \theta_\omega \boldsymbol{n}_\omega$, $\|\boldsymbol{n}_\omega\| = 1$. The rotation axis $\boldsymbol{\omega}$ is obtained by the least squares method with the performance function given by combining the relations of (4) or (5) with respect to the frame i and feature point j.

3. MODELING OF REBOUND

3.1 Rebound between the ball and table

Figure 5 shows the rebound of the ball from the table, where $(\boldsymbol{v}_b, \boldsymbol{\omega}_b)$ and $(\boldsymbol{v}'_b, \boldsymbol{\omega}'_b)$ are the translational and rotational velocities of the ball just before and after the rebound and Σ_B is the reference frame with the z-axis normal to the table. The simplest model of the rebound phenomenon is described by the equations of $v'_{bz} = -e_t v_{bz}$, $v'_{bx} = v_{bx}$ and $v'_{by} = v_{by}$, where e_t is the coefficient of restitution of the table in the z direction. In this model, it is assumed that there does not exist friction on the table. Therefore, the components x and y of the velocity $\boldsymbol{v}_b$ do not change. However, since there actually *exists the friction*, the velocity $\boldsymbol{v}'_b$ just after the rebound changes due to the friction and the rotational velocity $\boldsymbol{\omega}_b$ as shown in Fig. 6. The red and blue circles represent the cases of the top and back spins respectively and the ball velocities just before the rebound are the same. It is easily confirmed that the velocity v'_{bz} in the case of the back spin is greater than in the case of the top spin. In addition, the rotational velocity $\boldsymbol{\omega}'_b$ also changes due to the friction. In order to predict the ball trajectory after the rebound from the table, it is necessary to consider the friction.

For integrating the effect of the friction in the rebound model, it is very important to consider the *type of the contact* during the impact, i.e., the sliding and rolling contact. It can be determined which the contact is sliding or rolling, by using the contact velocity given by

$$\boldsymbol{v}_{bT} := [v_{bx}\ v_{by}\ 0]^{\mathrm{T}} + \boldsymbol{\omega} \times \boldsymbol{r} = \begin{bmatrix} v_{bx} - r\omega_{by} \\ v_{by} + r\omega_{bx} \\ 0 \end{bmatrix}, \tag{6}$$

where $\boldsymbol{r} := [0\ 0\ -r]^{\mathrm{T}} \in \mathbb{R}^3$ is the contact point of the ball from its center and $r \in \mathbb{R}_+$ is the ball radius. For the modeling, we make the following assumptions:

Assumption 1: During the impact of the rebound, the type of the contact between the ball and table is a point of contact. This means that any moment does not effect on the ball during the impact.

Assumption 2: The differences between the translational and angular momentums before and after the rebound equal the impulses at the rebound. Therefore, the impulse of the rotation is given by $\boldsymbol{r} \times \boldsymbol{P}$, where $\boldsymbol{P} \in \mathbb{R}^3$ is the impulse in the translational direction.

Assumption 3: The following simple bounce relationship in the z direction holds:

$$v'_{bz} = -e_t v_{bz} \tag{7}$$

Assumption 4: The impulse in the x and y directions $\boldsymbol{P}_{xy} := [P_x\ P_y\ 0]^{\mathrm{T}} \in \mathbb{R}^3$ is given by

$$\boldsymbol{P}_{xy} = -\lambda \frac{\boldsymbol{v}_{bT}}{\|\boldsymbol{v}_{bT}\|},\ 0 \le \lambda \le \mu |P_z|, \tag{8}$$

where μ is the dynamical coefficient of friction between the ball and table.

Assumption 5: The contact velocities $\boldsymbol{v}_b$ and $\boldsymbol{v}'_b$ just before and after the rebound are in the same direction. That is, the following relation holds:

$$\boldsymbol{v}'_{bT} = \nu \boldsymbol{v}_{bT},\ \nu \ge 0. \tag{9}$$

If $\nu \neq 0$, $\lambda = \mu |P_z|$.

Assumptions 4 and 5 are necessary to express the sliding and rolling contacts during the impact. Assumption 4 means that the impulse in the x and y directions is related to the one in the z direction as shown in Fig. 7 (a), where

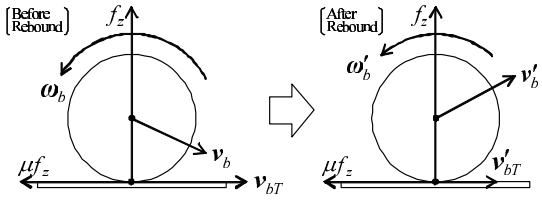

(a) Case where the contact is sliding during the impact

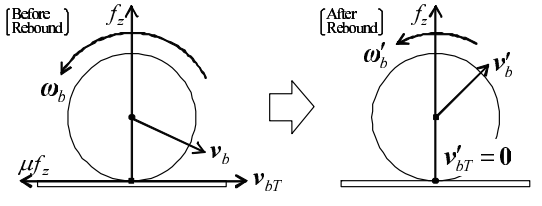

(b) Case where the contact is changed from sliding to rolling during the impact

Fig. 7 Sliding and rolling during the impact.

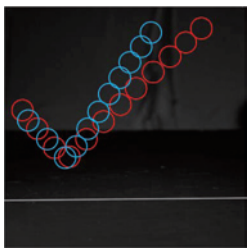

Fig. 6 Defference of $\boldsymbol{v}'_b$ when $\boldsymbol{\omega}_b$ is the top or back spin.

the friction force in the x and y directions is proportional to f_z with μ and its direction is the opposite one of $\boldsymbol{v}_{bT}$. λ in (8) is the magnitude of $\boldsymbol{P}_{xy}$ and is equal to or smaller than $\mu|P_z|$ because the contact can be changed from sliding to rolling during the impact as shown in Fig. 7 (b). Note that the static friction force does not work on the ball when the contact is rolling. Assumption 5 means that the contact velocity $\boldsymbol{v}'_{bT}$ after the rebound does not become negative because the rolling starts just after $\boldsymbol{v}'_{bT} = \boldsymbol{0}$. The condition of $\nu \neq 0$ means that the contact is sliding during the impact.

From Assumptions 1, 2, the following equations hold:

$$m\boldsymbol{v}'_b - m\boldsymbol{v}_b = \boldsymbol{P} \tag{10}$$

$$I\boldsymbol{\omega}'_b - I\boldsymbol{\omega}_b = \boldsymbol{r} \times \boldsymbol{P}, \tag{11}$$

where m and $I = \frac{2}{3}mr^2$ are the mass and moment of inertia. Combining (7) and (10) yields the relation in the z direction:

$$P_z = -m(1 + e_t)v_{bz}. \tag{12}$$

For deriving the relation in the x and y directions, the contact velocity $\boldsymbol{v}'_b$ after the rebound is calculated by the definition of (6) with (10), (11) and Assumption 4:

$$\boldsymbol{v}'_{bT} = -\lambda\left(\frac{1}{m} + \frac{r^2}{I}\right)\frac{\boldsymbol{v}_{bT}}{\|\boldsymbol{v}_{bT}\|} + \boldsymbol{v}_{bT}. \tag{13}$$

The contact velocity after the rebound, $\boldsymbol{v}'_{bT}$, has to satisfy (9) of Assumption 5. Substituting (13) into (9) yields

$$\nu = -\frac{\lambda}{\|\boldsymbol{v}_{bT}\|}\left(\frac{1}{m} + \frac{r^2}{I}\right) + 1. \tag{14}$$

It is sufficient to check whether ν of (14) is positive or not when the contact during the impact is supposed to be sliding, that is, $\lambda = \mu|P_z|$. Combining $\lambda = \mu|P_z|$, (12), $I = \frac{2}{3}mr^2$ and (14) leads to

$$\nu_s := 1 - \frac{5}{2}\mu(1 + e_t)\frac{|v_{bz}|}{\|\boldsymbol{v}_{bT}\|}, \tag{15}$$

which is defined as ν in the case of the sliding. It follows that (i) if $\nu_s > 0$, $\nu = \nu_s$ and $\lambda = \mu|P_z|$ (the case of the sliding); (ii) if $\nu_s \leq 0$, $\nu = 0$ (the case of the rolling).

Let us consider the sliding case of (i). Substituting (8) with $\lambda = \mu|P_z|$ and (12) into (10) and (11), we get the translational and rotational velocities after the rebound, $\boldsymbol{v}'_b$ and $\boldsymbol{\omega}'_b$, as the functions of those before the rebound:

$$\boldsymbol{v}'_b = \boldsymbol{A}_v\boldsymbol{v}_b + \boldsymbol{B}_v\boldsymbol{\omega}_b \tag{16}$$

$$\boldsymbol{\omega}'_b = \boldsymbol{A}_\omega\boldsymbol{v}_b + \boldsymbol{B}_\omega\boldsymbol{\omega}_b, \tag{17}$$

where

$$\boldsymbol{A}_v := \begin{bmatrix} 1-\alpha & 0 & 0 \\ 0 & 1-\alpha & 0 \\ 0 & 0 & -e_t \end{bmatrix}, \boldsymbol{B}_v := \begin{bmatrix} 0 & \alpha r & 0 \\ -\alpha r & 0 & 0 \\ 0 & 0 & 0 \end{bmatrix}$$

$$\boldsymbol{A}_\omega := \begin{bmatrix} 0 & -\frac{3\alpha}{2r} & 0 \\ \frac{3\alpha}{2r} & 0 & 0 \\ 0 & 0 & 0 \end{bmatrix}, \boldsymbol{B}_v := \begin{bmatrix} 1-\frac{3\alpha}{2} & 0 & 0 \\ 0 & 1-\frac{3\alpha}{2} & 0 \\ 0 & 0 & 1 \end{bmatrix}$$

$$\alpha := \mu(1 + e_t)\frac{|v_{bz}|}{\|\boldsymbol{v}_{bT}\|}. \tag{18}$$

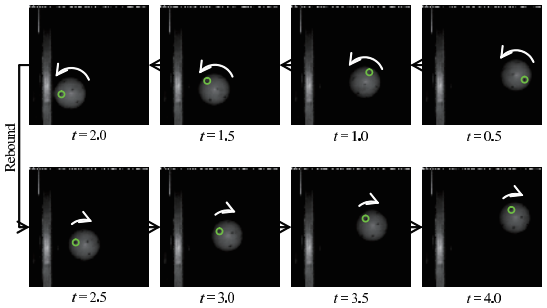

Fig. 8 Rebound of the ball from the racket rubber.

Next consider the rolling case of (ii). From $\nu = 0$ and (14), λ is given by

$$\lambda = \frac{2}{5}m\|\boldsymbol{v}_{bT}\|. \tag{19}$$

By the similar calculation of the case (i) with (19), we get the coefficient matrices of (16) and (17) as follows:

$$\boldsymbol{A}_v := \begin{bmatrix} \frac{3}{5} & 0 & 0 \\ 0 & \frac{3}{5} & 0 \\ 0 & 0 & -e_t \end{bmatrix}, \boldsymbol{B}_v := \begin{bmatrix} 0 & \frac{2r}{5} & 0 \\ -\frac{2r}{5} & 0 & 0 \\ 0 & 0 & 0 \end{bmatrix}$$

$$\boldsymbol{A}_\omega := \begin{bmatrix} 0 & -\frac{3}{5r} & 0 \\ \frac{3}{5r} & 0 & 0 \\ 0 & 0 & 0 \end{bmatrix}, \boldsymbol{B}_v := \begin{bmatrix} \frac{2}{5} & 0 & 0 \\ 0 & \frac{2}{5} & 0 \\ 0 & 0 & 1 \end{bmatrix}. \tag{20}$$

3.2 Rebound between the ball and racket rubber

Fig. 8 shows an example of the rebound of the ball from the racket rubber. The green circles represent the same point on the ball. It is confirmed that the rotational velocity about the axis normal to the image plane changes to the *inverse* direction after the rebound. This imply that the contact velocities between the ball and the rubber before and after the rebound are opposite each other. This can not be expressed by considering only the friction and is the specific phenomenon in the case of the rubber due to the storage of its elastic energy. In order to achieve desired ball trajectory after the rebound from the racket, it is necessary to consider this phenomenon.

The left of Fig. 9 shows the rebound of the ball from the racket rubber, where the meanings of the variables are the same as in Section 3.1 with respect to the racket frame Σ_R attached to the racket as the z-axis normal to

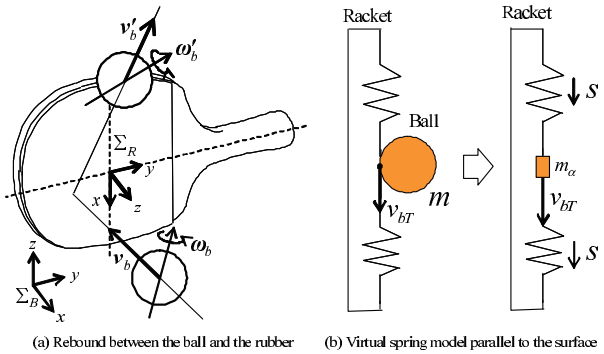

(a) Rebound between the ball and the rubber (b) Virtual spring model parallel to the surface

Fig. 9 The rebound between the ball and the rubber.

the surface. In order to express the effect of the elasticity parallel to the surface, we model the tangent motion of the racket rubber as the motion of the virtual mass m_α with the spring k_s and the distance $\boldsymbol{s}(t) \in \mathbb{R}^3$ as shown in the right of Fig. 9. Note that m_α is the equivalent mass consisting of the mass of the ball and the deformed area of the rubber.

For the modeling, we make the following assumptions:

Assumption 6: The rebound in the z direction does not cause any effect on the ones in the x and y directions.

Assumption 7: The kinetic energy of the virtual mass is conserved as the elastic energy without the dissipation. $\boldsymbol{s}_{\max} \in \mathbb{R}^3$ is the maximum displacement of the virtual mass with the same direction of the contact velocity $\boldsymbol{v}_{bT}$.

Assumption 8: The elasticity of the rubber is uniform in the x and y directions. This means that the stiffness k_s is same in any x and y directions.

Assumption 9: The time rate of $\boldsymbol{s}(t)$ is a constant during the impact.

Assumptions 1–4 are also assumed to hold here.

From Assumptions 7 and 8, the following energy conservation holds:

$$\frac{1}{2} m_a \|\boldsymbol{v}_{bT}\|^2 = \frac{1}{2} k_s \|\boldsymbol{s}_{\max}\|^2. \tag{21}$$

(21) is solved with respect to $\boldsymbol{v}_{bT}$ as

$$\boldsymbol{s}_{\max} = \sqrt{\frac{\alpha}{m_\alpha}} \boldsymbol{v}_{bT}. \tag{22}$$

By (22) and Assumption 9, the impulse $\boldsymbol{P}_{xy} \in \mathbb{R}^3$ in the x and y directions is obtained as

$$\boldsymbol{P}_{xy} = \int_0^T -k_\alpha \boldsymbol{s}(t) dt = -k_p \boldsymbol{v}_{bT},\ k_p := \frac{T}{2} \sqrt{m_\alpha k_\alpha}, \tag{23}$$

where $T \in \mathbb{R}_+$ is the time interval of the impact. From Assumption 1–3 and 6, the equations of (10), (11) and (12) also hold here. Combining (23), (10), (11) and (12), we get the translational and rotational velocities after the rebound, $(\boldsymbol{v}_b', \boldsymbol{\omega}_b')$, are given by the same functional relationships as (16) and (17) with the coefficient matrices as follows:

$$\begin{aligned}
&\boldsymbol{A}_v := \begin{bmatrix} 1-k_{pv} & 0 & 0 \\ 0 & 1-k_{pv} & 0 \\ 0 & 0 & -e_r \end{bmatrix}, \boldsymbol{B}_v := k_{pv} \begin{bmatrix} 0 & 0 & 0 \\ 0 & 0 & r \\ 0 & -r & 0 \end{bmatrix} \\
&\boldsymbol{A}_\omega := k_{p\omega} \begin{bmatrix} 0 & 0 & 0 \\ 0 & 0 & -r \\ 0 & r & 0 \end{bmatrix}, \boldsymbol{B}_v := \begin{bmatrix} 1 & 0 & 0 \\ 0 & 1-k_{p\omega} r^2 & 0 \\ 0 & 0 & 1-k_{p\omega} r^2 \end{bmatrix} \\
&k_{pv} := \frac{k_p}{m},\ k_{p\omega} := \frac{k_p}{I},
\end{aligned} \tag{24}$$

where e_r is the coefficient of restitution of the rubber.

Table 1 Verification of the table rebound model

No.	$(v_{bx}, v_{bz}, \omega_{by})$	$(v_{bx}', v_{bz}', \omega_{by}')$	Model
1	$(-2.8, -3.3, 279)$	$(-3.8, 3.0, 196)$	$(-4.0, 3.1, 199)$
2	$(-3.6, -2.1, 216)$	$(-3.8, 2.0, 209)$	$(-3.8, 2.0, 194)$
3	$(-4.1, -2.2, -286)$	$(-3.1, 2.0, -224)$	$(-3.0, 2.1, -206)$
4	$(-3.8, -1.8, -216)$	$(-3.0, 1.7, -161)$	$(-2.9, 1.7, -150)$
5	$(-2.7, -2.2, -170)$	$(-1.9, 1.9, -100)$	$(-1.7, 1.9, -90.6)$
6	$(-2.6, -2.2, -165)$	$(-1.7, 2.0, -93.7)$	$(-1.5, 2.1, -83.9)$

4. PARAMETER IDENTIFICATION AND MODEL VERIFICATION

The coefficient of restitution of the table e_t can be calculated as

$$e_t = \sqrt{\frac{h_2}{h_1}}, \tag{25}$$

where h_1 and h_2 are the first and second heights of the dropped ball. e_t is identified as $e_t = 0.93$ by meaning 25 data. The dynamical friction coefficient μ is estimated as $\mu = 0.25$ by measuring the drastic changed value of the spring balance instrument at the sliding where the weighted ball on the table with the weight 2.0[kg] is pulled.

The experimental verification of the rebound model of the table is shown in Table 1. The experimental data are limitted to the cases of the pure top spin ($\omega_{by} < 0$) or pure back spin ($\omega_{by} > 0$) with $v_{by} \simeq 0$. Hence (v_{bx}, v_{bz}) [m/s] and ω_{by} [rad/s] are only shown in Table 1. The number 1 and 2 are the cases of the top spin and the number 3–6 are the cases of the back spin. The errors of the velocity and rotation are $e_v = 1.0$–11.1 [%] and $e_\omega = 1.5$–10.5 [%]. There is a little big error of the order of 10 [%] since the changes between frames of the data may be hidden in the quantization errors. These was happened in the cases where the spins are smaller than the ones of the other data. Except for these results, the errors are smaller than 10 [%]. Therefore, this verification can show the validation of the model.

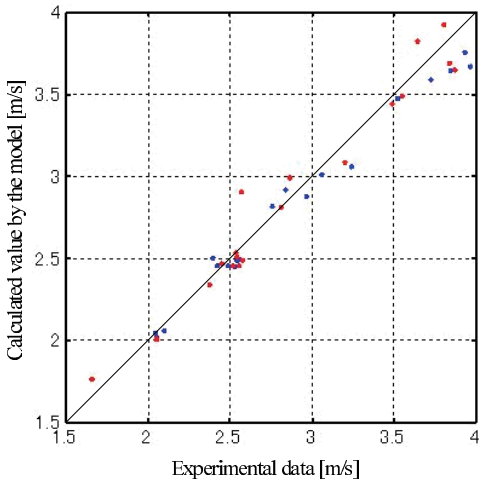

Fig. 10 Verification of v_{bz}' of the rubber case.

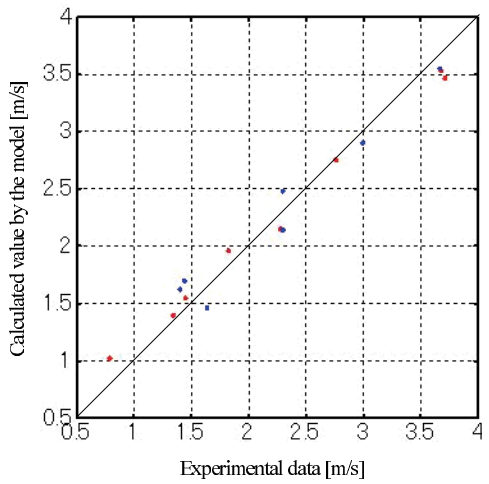

Fig. 11 Verification of v'_{bx} of the rubber case.

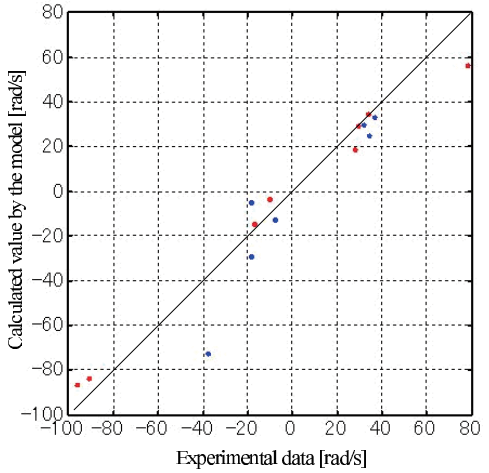

Fig. 12 Verification of ω'_{by} of the rubber case.

The experimental data in the case of the rubber are also only the pure top or back spin. The parameters are indentified as $e_r = 0.503$, $k_{pv} = 0.68$ and $k_{p\omega} = 2.25 \times 10^3$ [1/m^2]. Figures 10–12 show the verifications of v'_{bz}, v'_{bx} and ω'_{by}, which are the translational and rotational velocities after the rebound normal and parallel to the rubber. The red data are used for the identification of the parameters and the blue data are used for the verification. The solid line represents the set of the points where the values of the experiment and model equal each other. It is confirmed that the parameters are identified well because the red data are close to the solid line. It is also confirmed that the blue data are close to the solid line and are distributed around the one with the almost same variance as the red data. This can show the relevance of the model of the rubber.

Table 2 shows the experimental data of the contact velocities before and after the rebound and the ones after the rebound which are calculated by the model. It is confirmed that the calculated velocities are in the opposite directions of the velocities before the rebound and close to the velocities after the rebound. Therefore, the proposed model can represent the specified effect of the rubber.

Table 2 Verification of the contact velocity

No.	Before the rebound	After the rebound	Calculated by Model
1	−3.79	2.35	2.21
2	−3.87	2.12	2.26
3	−3.77	2.04	2.20
4	−3.92	2.03	2.29
5	−3.68	2.02	2.15
6	−3.74	2.37	2.18

5. CONCLUSIONS

We have modeled the rebound phenomenon between a ping-pong ball and the table/racket rubber. In the model between the ball and racket rubber, it was assumed that the kinetic energy of the contact velocity was stored as the potential energy due to the elasticity of the rubber. This assumption led to that the impulse in the horizontal direction was proportional to the contact velocity. The vertical and horizontal COR in the models of the table and rubber were identified with the measured velocity and spin of the ball by high-speed vision sensors. The models were verified by other experimental data.

REFERENCES

[1] R. Garwin, “Kinematics of an ultraelastic rough ball,” *Am. J. Phys.*, Vol.37, pp.88–92 1969.

[2] H. Brody, “That’s how the ball bounces,” *Phys. Teach.*, Vol.22 pp.494–497, 1984.

[3] Kanji Shibukawa, *Dynamics of Physical Exercise*, Daishukanshoten, 1969 (in japanease).

[4] R. Cross, “Effects of friction between the ball and strings in tennis,” *Sports Eng.*, Vol.3, pp.85–97, 2000.

[5] R. Cross, “Measurements of the horizontal coefficient of restitution for a superball and a tennis ball,” *Am. J. Phys.*, Vol.70, No.5, pp.482–489, 2001.

[6] R. Cross, “Bounce of a spinning ball near normal incidence,” *Am. J. Phys.*, Vol.73, No.10, pp.914–920, 2005.

[7] R. Cross, “The bounce of a ball,” *Am. J. Phys.*, Vol.67, No.3, pp.222–227, 1999.

[8] Y. Kawazoe and D. Suzuki “Prediction of Racket Performance Based on the Table Tennis Impact Analysis,” *Porc. Dynamics and Design Conf.*, 218, 2002 (in japanease).

[9] B. K. Ghosh, N. Xi and T. J. Tarn, *Control in Robotics and Automation: Sensor-Based Integration*, Academic Press, 1999.

[10] R. M. Murray, Z. Li and S. S. Sastry, *A Mathematical Introduction to ROBOTIC MANIPULATION*, CRC Press, 1994.